J. Fluid Mech. (1986), *vol.* 170, *pp.* 319–337
Printed in Great Britain

On the population of the metastable states behind unstable shock waves in ionizing argon

By A. F. P. HOUWING, T. J. McINTYRE, P. A. TALONI AND R. J. SANDEMAN

Department of Physics and Theoretical Physics, Australian National University, Canberra, Australia

(Received 19 November 1985 and in revised form 3 March 1986)

Experiments are described in which the populations of metastable levels in ionizing argon are measured through spatially resolved hook interferometry. The results are compared with the present model for shock-induced ionization and a recently proposed mechanism to explain observed flow instabilities. It is found that the experimental measurements support the presently accepted model, which states that electron–atom collisions play the dominant role in the excitation process, but contradicts recent proposals which predict a rapid build-up of anomalously high metastable populations through atom–atom collisions.

1. Introduction

Over the past twenty-five years, a considerable amount of work has been done on the study of the reaction mechanism for ionization behind shock waves in monatomic gases, with particular emphasis on argon. These investigations relied on the production of a plane shock wave followed by a one-dimensional relaxation zone which could be studied by a variety of methods. (See, for example, Petschek & Byron 1957; Harwell & Jahn 1964; Kelly 1966; McLaren & Hobson 1968; Wong & Bershader 1966; Oettinger & Bershader 1967; Demmig 1977). Most of these studies were made for shock-wave Mach numbers M_s ranging from 10 to 14. Other studies, however, showed that for larger Mach numbers the relaxation zone was not always one-dimensional. Using Mach Zehnder interferometry, Bristow & Glass (1972) found that, for $M_s = 17$ and initial gas pressure $p_0 = 2.8$ Torr, the translational shock front was no longer plane, while sinusoidal-type oscillations perturbed the relaxation zone and the quasi-equilibrium region. They found that it was possible to remove these disturbances and stabilize the shock wave by adding 0.4 % (by partial pressure) hydrogen to the argon test gas. In addition, they noted that the hydrogen impurity significantly reduced the length of the relaxation zone. This reduction of the relaxation length was accounted for kinetically, but the reason why hydrogen impurities stabilized the flow was not understood. Nonetheless, since the low impurity concentration changed only the reaction rates while not causing any significant change in the quasi-equilibrium values, their observations demonstrated that the instability was most likely caused by the relaxation process.

A number of different theories have been put forward by various authors to explain the observation of shock-wave instability. Many of these were in existence before instabilities were observed in shock waves in argon, and were attempts to explain the instabilities in detonation waves (see Fickett & Davis 1979). Freeman (1955) and Whitham (1956) treated the two-dimensional problem of an initially plane shock

wave in an ideal gas. The shock was considered to be a discontinuity surface and given a small initial disturbance. They found that the perturbation decayed like $t^{-\frac{1}{2}}$ for a weak shock and $t^{-\frac{3}{2}}$ for a strong shock. These predictions were verified experimentally in shock-tube flows where, for an ideal gas, the shock wave became planar within 4 to 8 tube diameters from the diaphragm (Glass & Patterson 1955). This and other work (Freeman 1957; Lapworth 1959; von Moorheim & George 1975) showed that shock waves in perfect gases were inherently stable. For a medium with an arbitrary equation of state, however, D'yakov (1954) found stability criteria in terms of the gradient of the Hugoniot curve and the slope of the Rayleigh line. His analysis was applicable to non-ideal gases which undergo dissociation or ionization, but it assumed that all reaction rates were infinitely fast. Consequently it was not applicable to situations where the instability was shown to originate in the reaction zone. A more detailed analysis that does take into account the rate for a simple reaction system is that due to Erpenbeck (1963, 1969). His treatment was very successful in predicting the stability of detonation waves, but had only limited applicability to endothermic reactions (i.e. dissociation and ionization). Baryshnikov & Skvortsov (1979), however, pointed out that even though the overall process for a particular reaction system is endothermic, it is possible that an intermediate stage is exothermic and sufficiently energetic to destabilize the flow. They arrived at a set of hydrodynamic stability conditions by using an analysis that is similar to D'yakov's method but incorporates the relaxation rate for a simple reaction. Mishin *et al.* (1981) suggested that for ionizing gases the exothermic stage necessary for instability comes about in the following way. During the early stages of ionization, atom–atom collisions might be responsible for populating metastable states at excitation temperatures above the translational temperature of the atoms. It was suggested that the excess energy is stored in these metastable atoms and later released through superelastic collisions, which are likened to exothermic chemical reactions. Yushchenkova (1980) used a set of rate equations to determine how rapidly these metastable states are populated and predicted that maximum populations are achieved almost immediately behind the translational shock front. This, however, is in contradiction with the accepted mechanism for ionization in which the transition from the ground state to excited levels is considered to be the rate-determining step. In an attempt to clarify this apparent contradiction, the present study deals basically with: (i) interferometric studies of flow stability in ionizing argon with a view to comparing the observations with the model proposed by Baryshnikov & Skvortsov and Mishin *et al.*; and (ii) an experimental determination of the populations of metastable and non-metastable excited states using hook interferometry to compare with values predicted by Yushchenkova.

2. Theoretical considerations

2.1. *Ionizing-gas flow*

Physical models to describe the kinetics for ionization have been proposed by several investigators, principally Petschek & Byron (1957), Bond (1957), Weymann (1958) and Harwell & Jahn (1964). Further studies have been reported by Brown & Mullaney (1964), Morgan (1964), Wong & Bershader (1966), Oettinger & Bershader (1967) and Glass & Liu (1978). In particular, Harwell & Jahn were able to establish the electron density distribution in the region immediately behind the translational shock front, and thus lend support to the two-stage atom–atom inelastic collision mechanism. This mechanism

$$A + A \rightarrow A^* + A, \quad A^* + A \rightarrow A^+ + e^- + A,$$

proposed that excitation of the atom preceded its ionization and was shown by Weymann to be more efficient than the direct ionization process. Harwell & Jahn's results supported this proposal, since they determined an activation energy of 11.5 eV which corresponded to the first excited state of argon. It is important to note (prior to the discussion on the population of metastable states) that the probability for subsequent ionization of excited states is several orders of magnitude larger than the probability of excitation from the ground state. Consequently, as pointed out by Wong & Bershader, the initial step of the two-step process is the rate-controlling one, and there is no net accumulation of atoms in the excited states. In the plasma, the heavy particles (atoms and ions) and the electrons separately experience sufficiently numerous collisions to result in independent Maxwellian distributions of their thermal energies at atom and electron temperatures, T_A and T_e, respectively. Since the cross-section for energy transfer between atoms and electrons through elastic collisions is relatively low, these two temperatures remain quite different throughout most of the relaxation zone. In particular, since the electrons have lost much of their kinetic energy in overcoming the ionization potential, T_e is initially much less than T_A. After a sufficiently long time, however, the free electrons increase their thermal energy through elastic collisions with the heavy particles. At these higher energies the electrons can interact inelastically with the atoms, exciting and ionizing them and thereby increasing the number of free electrons in the plasma. When sufficient electrons are available, the relatively large electron–atom cross-section coupled with the high mobility of the electrons causes these electron–atom collisions to become the dominant mechanism for ionization. The dependence of this mechanism on electron temperature and number density means that an avalanche effect takes place in a relatively narrow region known as the electron-cascade front, where the plasma parameters very rapidly reach their quasi-equilibrium values.

Since the first excited level of the argon atom is 11.5 eV above the ground state and the undisturbed ionization limit is 15.8 eV, adequate inelastic collisions are assumed to occur between the free electrons and the excited atoms to maintain the population of all excited levels in a Boltzmann distribution based on the electron temperature throughout the relaxation zone (see Bates, Kingston & McWhirter 1962; Byron, Stabler & Bortz 1962; Oettinger & Bershader 1967). On the basis of this distribution, Oettinger & Bershader derive a 'modified' Saha equation relating the population of an excited state q to the electron number density and temperature. This equation is

$$n(q) = \frac{n_e^2 h^3}{2(2\pi m_e kT_e)^{\frac{3}{2}}} \frac{g(q)}{Q_i(T_e)} \exp\left[\frac{I - E_q}{kT_e}\right], \tag{1}$$

where $n(q)$ is the number density of atoms in the excited state q; n_e is the electron number density; $g(q)$ is the degeneracy of state q; Q_i is the partition function of the ions; I is the ionization potential for the atom and E_q is the excitation energy of the state q. The ion partition function is assumed to be

$$Q_i(T_e) = 4 + 2\exp\left(\frac{-2060}{T_e}\right), \tag{2}$$

that is, the ion is considered to be only in its two ground states. Equation (1) implies that there is no significant population of the metastable states until a significant electron population has been reached, i.e. at the electron-cascade front. It is worth noting that the above equations assume a Maxwellian velocity distribution for the electrons. However, recent work by Meyer-Prüssner (1983) and Demmig (1983) suggests that, in the early stages of ionization, the distribution more closely

represents a 'truncated Maxwellian'. It is believed that when the electron density is low, the frequency of electron–electron collisions is not sufficient to replenish the high-energy Maxwell tail which is being depleted by inelastic electron–atom collisions. Consequently, one can expect some deviation from (1). Meyer-Prüssner takes into account the effect of the non-Maxwellian distribution on the excited states and predicts that their populations can be two orders or magnitude lower in the relaxation zone. However, the velocity distribution approaches a true Maxwellian near the electron-cascade front. Consequently (1) can be regarded as valid at the cascade front and in the quasi-equilibrium region. Once the plasma parameters have reached their quasi-equilibrium values behind the electron-cascade front, the high electron number densities give rise to radiation losses through *bremsstrahlung* and radiative recombination. This loss process is slow when compared to the original ionization process, and consequently takes place over a region which is large compared to the ionization–relaxation zone. Furthermore, the elastic energy transfer and recombination reactions are sufficiently fast to maintain thermal and chemical equilibrium during the cooling process.

2.2 *Anomalous relaxation*

The theory of anomalous relaxation, proposed by Baryshnikov & Skvortsov (1979) and Mishin *et al.* (1981), considers a series of chemical reactions in the relaxation zone, which lead to an exothermic stage in an overall endothermic reaction sequence. These authors suggest that, if the release of energy is sufficiently large, it can amplify perturbations in the post-shock flow. They propose that this energy release can come about as follows:

(i) storage of kinetic energy of the shock wave into highly excited internal energy states of the particles;

(ii) an accumulation of these excited particles in the flow;

(iii) a transfer of the energy into a form suitable for deactivation; and

(iv) rapid deactivation by superelastic collisions.

The particle state which is important in the energy storage is proposed to be different for different types of gases. For monatomic ionizing gases, it is suggested that energy is stored in electronic levels of the atom, whereas for molecular gases it is suggested that energy is stored in highly excited vibrational states or in chemical bonds. For an instability to occur from the above process, the flow conditions need to be of a suitable form. The first step in the process requires a sufficiently strong shock that will impart enough energy to excite the particles to these levels. It follows therefore that there is a minimum shock strength below which sufficient quantities of excited particles will not be formed. Mishin *et al.* suggest that the density of the gas is also crucial in the reaction sequence. If the density is too low, deactivation will not occur at a sufficient rate to drive the instability and the internal energy may eventually be lost as emission. If the density is too high, collisions will rapidly bring the flow to equilibrium and no instability results. This point appears to be consistent with observations made by Griffiths, Sandeman & Hornung (1976) who found that, for Mach numbers comparable with Bristow & Glass's (1972) experiments but at higher densities, shock waves were stable. Furthermore it follows that impurities (such as hydrogen) which have a much larger deactivation cross-section than the test gas would prohibit a build-up of excited particles. This explanation, if correct would be consistent with the observations made by Bristow & Glass and Glass & Liu (1978). The second step in the process requires that these excited states be long lived, such as metastable levels in an atom. The third step requires the existence of a suitable

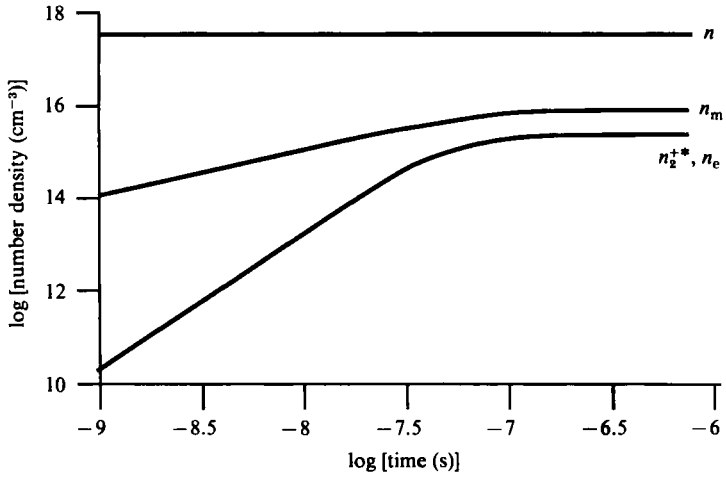

FIGURE 1. Numerical solution of Yushchenkova's (1980) rate equations, n, n_m, n_e, n_2^{+*}: number density of argon atoms, metastable particles, electrons and molecular ions, respectively. Conditions correspond to $p_0 = 10$ Torr, $M_s = 14.6$.

particle state for deactivation. The fourth step requires this state to have a large reaction cross-section so that the reaction is sufficiently intense. The result is a deactivation that increases the Maxwellian temperature of the gas, which in turn increases the superelastic collision rate to release even more energy into the flow. Thus for monatomic gases, for example, provided sufficient metastable particles are present, the flow will become unstable to perturbations in the gas temperature.

2.3. *Anomalous relaxation in ionizing gases*

To consider anomalous relaxation in a particular gas, it is necessary to establish the existence of an exothermic reaction sequence. This was done by Yushchenkova (1980), who suggests a reaction sequence involving metastable atoms and molecular ions. The molecular ions (the proposed form for deactivation), are supposedly formed by atom–atom collisions, and then removed by collisions with electrons. Although a large variety of reactions may affect the concentrations of these particles, Yushchenkova proposes only the following in an approximate formulation of the problem:

$$A + A \rightarrow A^m + A \tag{0}$$

$$A^m + A^m \rightarrow A_2^{+*} + e^- \tag{I}$$

$$A_2^{+*} + e^- \rightarrow A^{**} + A \rightarrow A^m + A + E + h\nu. \tag{II}$$

Reaction (0) is necessary for the formation of metastable particles, A^m; while reaction (I) generates excited molecular ions, A_2^{+*}, suitable for the deactivation which occurs via reaction (II). In this last reaction, A^{**} represents an atom excited to a level above the metastable state; E is the energy released through collisional de-excitation of the molecular ion; while $h\nu$ represents the energy lost via radiative de-excitation of A^{**}. For these reactions Yushchenkova presents a set of rate equations which she then uses to determine the number densities of the electrons, metastable atoms and molecular ions. Numerical solutions of these equations for our experimental conditions are plotted in figure 1. From this figure we note that the

metastable population is predicted to rise rapidly to a large value (approximately 2 % of the ground-state population) in a very short time ($< 10^{-7}$ s). This anomalously high population can be shown to correspond to an excitation temperature of 23000 K, which is close to the Maxwellian temperature (19600 K) of the heavy particles behind the translational shock. This is, of course, in contradiction to the model discussed in §2.1, which predicts that the excitation temperature will equal the electron temperature.

Yushchenkova proposes that the above reaction sequence occurs within the relaxation zone and causes the shock-wave instability, and presents some experimental work to support her proposal. She points out that it is possible to study the kinetics of the reactions by introducing known quantities of metastable particles ahead of the shock and monitoring the concentration of reaction products behind the shock through emission measurements. These emission measurements were obtained by adding a small amount of xenon to the flow. The reaction,

$$Ar_2^{+*} + Xe \rightarrow Ar\,Xe^{+*} + Ar,$$

enabled indirect measurements of the molecular ion Ar_2^{+*} concentrations by monitoring the Ar Xe^+ spectral band. In this manner, Yushchenkova studied the kinetics of reactions (I) and (II) in a 'low-density plasma-dynamic stream apparatus', in which shock waves could be produced. These 'streams' had high concentrations of excited particles, and simulated the state of argon plasmas in shock waves, for $10 < M_s < 25$, through supersonic flow over bluff bodies or by the interaction of the plasma flow and a colliding gas flow. She supports her proposal as far as reactions (I) and (II) are concerned. However, since metastables were introduced artificially, she was not able to demonstrate that reaction (0) occurs at a sufficient rate (if at all) to produce the required number of metastable particles, in a flow where such particles are initially absent. Consequently the present work studies this reaction by measuring the population of the metastable states through spatially resolved hook interferometry.

2.4. *Hook interferometry*

Hook interferometry is a technique for measuring the product of the population of an atomic level and the oscillator strength of an absorption transition from that level. It relies on the dispersion of the atoms near the transition. By combining an interferometer with a spectrograph and with suitable adjustment of the interferometer, the white-light interference fringes observed at the spectrograph image plane form local maxima and minima, or hooks, on either side of the line. The spectral separation of these hooks is proportional to the square-root of the number density of the absorbing atoms and the oscillator strength of the transition. In our experiment, this technique is used to measure the number density of atoms in metastable and non-metastable levels with known oscillator strengths. Some of the transitions studied, however, have very low oscillator strengths, resulting in very small hook spacings, and the hook vernier method was used to improve the accuracy of some of these measurements. A detailed analysis of hook interferometry is given by Marlow (1967), while the hook vernier method is presented by Sandeman (1979). We present only the equations which are pertinent to our measurements.

Figure 2 is a qualitative representation of interference fringes near an absorption line as seen in the exit plane of a spectrograph. The hook width Δ is related to the population of the lower state N_i of the transition λ_{ij} by the expression

$$\Delta^2 = \left(\frac{r_0}{4\pi K}\right) N_i f_{ij} L \lambda_{ij}^3, \tag{3}$$

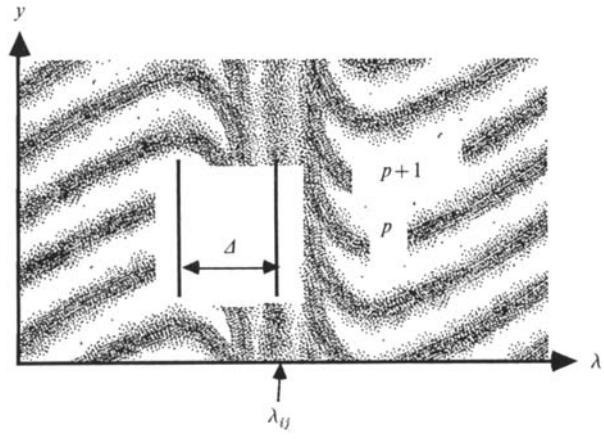

FIGURE 2. Section of a hook spectrum. λ_{ij}, line centre; Δ, hook separation from line centre.

where r_0 is the classical electron radius; f_{ij} is the oscillator strength of the transition; L is the optical pathlength; and K is the hook constant. In arriving at (3), it is assumed that λ_{ij} is sufficiently far from adjacent transition lines to be unaffected by their dispersion. In the absence of hooks, K is given by

$$K = -\lambda\left(\frac{\partial p}{\partial \lambda}\right)_{y\,=\,\text{const}},$$

where p is the order of the interference fringes. Rearranging (3), one can find a value for N_i once Δ is known. If the entrance slit of the spectrometer is imaged into the relaxation zone, then (3) will yield spatially resolved values for N_i along the slit image (see Sandeman & Ebrahim 1977). The hook vernier method relates the hook separation Δ to the fringe shift δp between the two hook positions at constant y on either side of the transition line, through the equation

$$\Delta = \frac{(p_{\mathrm{L}} - p_{\mathrm{R}})\,\lambda_{ij}}{4K}, \tag{4}$$

where the subscripts L and R refer to the left-hand and right-hand hooks, respectively, p_{L} and p_{R} being non-integral fringe orders measured at the same value of y. The above equation can be shown to be equivalent to the hook vernier equation derived by Sandeman if our Δ is identified with his Fx_{h} and our $p_{\mathrm{L}} - p_{\mathrm{R}}$ is identified with his n; with his Δ_y put equal to zero, since the fringe numbers of our left- and right-hand hooks were determined at constant y. The main advantage in using the vernier method is evident when one makes an estimate of the errors involved in the two different methods. This was done by Sandeman who showed that, for a particular example, the relative error in a measurement involving the vernier method was approximately one-quarter of that obtained through the conventional method.

3. Experimental arrangement

For the purpose of making direct comparisons with existing data on shock-wave stability in ionizing argon, it was decided to use conditions similar to those reported by Glass & Liu (1978). This was achieved by operating the ANU double-diaphragm shock tube to produce shock waves with $13 < M_{\mathrm{s}} < 18$ travelling into argon at initial

pressure 2.8 Torr $\leqslant p_0 \leqslant$ 10 Torr. The shock-tube facility, which is described by Sandeman & Allen (1971), can be operated in either 'double-diaphragm' or 'single-diaphragm' mode and is capable of producing shock waves with Mach numbers as high as 50. For the present investigation, however, it was only necessary to use the single-diaphragm mode to achieve the required Mach-number range. To obtain test-gas purity levels which were consistent with those reported by Glass & Liu, a silicone-oil diffusion pump backed by a conventional rotary vacuum pump was used to evacuate the shock-tube system to less than 10^{-4} Torr, at an outgassing rate of about 10^{-5} Torr/min. To further improve the purity level, the shock tube was first evacuated to below 10^{-4} Torr, then filled with 10 Torr argon, before re-evacuating to 10^{-4} Torr and then refilling to the required pressure of argon. The argon used had a purity better than 99.996 % by volume. The tube was filled to the desired pressure, as measured by a thermistor gauge, approximately two minutes before each shot to minimize outgassing effects. The uncertainty in shock-tube filling pressure was ± 0.5 Torr.

To fulfil the aims presented in the introduction, three different arrangements were used. The first involved using a Mach Zehnder interferometer, together with an exploding-wire light source and streak camera to produce time-resolved interferograms of the shock, relaxation zone and electron-cascade front. In the second method, the exploding wire was replaced by a nitrogen-laser-pumped-dye laser and the streak camera was replaced by a spectrometer to produce spatially resolved hook interferograms. The third method was very similar to the second, in that the optical arrangement was for spatially resolved hook interferometry. However, the nitrogen-laser-pumped-dye laser (N_2LPDL) was replaced by a coaxial flash-lamp-pumped-dye laser (FLPDL), which was in turn used to pump an external fluorescing source with output in the near infra-red. The FLPDL was set up to oscillate broadband at 650 nm using Rhodamine 640 to give maximum pumping efficiency of the infra-red dyes.

For the argon atom, there are two metastable levels (see Meissner & Graffunder 1927; Phelps & Molner 1953), these being the $1s_3$ and $1s_5$ energy levels (Paschen notation as used by Meissner 1926). Thus in order to determine the density of the metastable particles, it is necessary to measure and then add together the populations of these states. This is best achieved through studying transitions with sufficiently large oscillator strengths. Unfortunately, the strongest transitions occur in the near infra-red, were the output power of the N_2LPDL is relatively weak. This is a consequence of the fact that near infra-red dyes have relatively weak absorption at the wavelength of the nitrogen pump laser (337 nm) (see Pierce & Birge 1982). Because of this limitation, we were able to study the population of only the $1s_5$ level with the N_2LPDL. However, both levels could be studied with the FLPDL.

The transition lines used to measure the $1s_3$ and $1s_5$ populations were the $\lambda_{ij} = 696.543$; 763.511; 772.376; and 772.421 nm lines corresponding to the $1s_5$–$2p_2$; $1s_5$–$2p_6$; $1s_5$–$2p_7$; and $1s_3$–$2p_2$ transitions. These lines have oscillator strengths of $f_{ij} = 0.029 \pm 0.007$; 0.239 ± 0.060; 0.0306 ± 0.0077; and 0.341 ± 0.085 respectively (Weise, Smith & Miles 1969). In order to determine whether or not the populations of the metastable levels behaved significantly differently from those of the non-metastable levels, the $1s_2$ and the $1s_4$ excited states were also studied for comparison. The populations of these states were measured through the 738.398, 750.387 and 751.465 nm lines, corresponding to the $1s_4$–$2p_3$; $1s_2$–$2p_1$; and $1s_4$–$2p_5$ transitions. For these lines, $f_{ij} = 0.119 \pm 0.029$; 0.133 ± 0.033 and 0.121 ± 0.030 respectively. By selecting appropriate concentrations for different dyes it was possible to achieve spectral coverage over most of the desired wavelengths: 1.1×10^{-3} M Nile Blue in

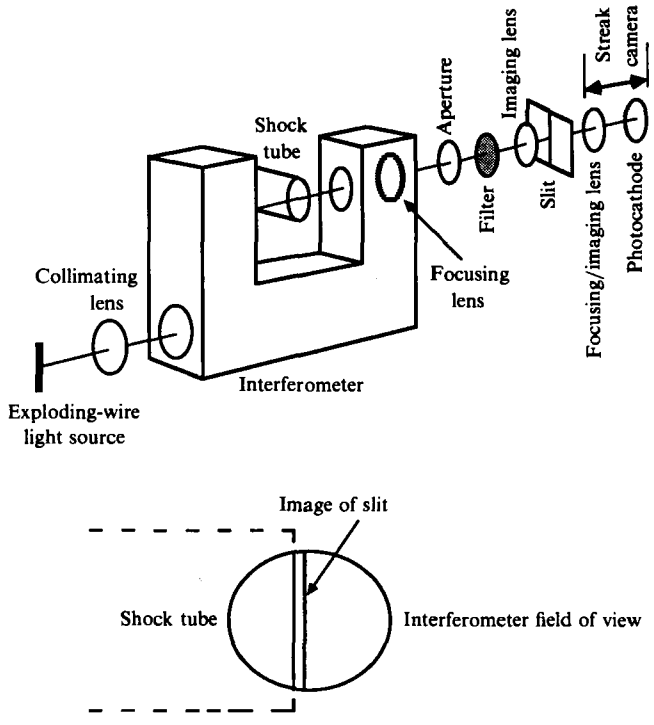

FIGURE 3. Optical arrangement for time-resolved flow visualization and interferometer field of view.

ethanol for $\lambda_{ij} = 696.543$ nm; and (1 to 3.5) $\times 10^{-4}$ M DOTC in ethyl glycol for the 730–780 nm range. The latter dye was particularly useful since it covered transitions from each of the two metastable levels ($1s_5$–$2p_6$, $1s_5$–$2p_7$ and $1s_3$–$2p_2$), and thus allowed the populations of these levels to be studied simultaneously.

The optical arrangement for flow visualization is illustrated in figure 3. The exploding wire provided an intense source of light lasting about 50 μs. This light was collimated through a Carl Zeiss Mach Zehnder interferometer aligned across the end of the shock tube. Zero-order white-light fringes, localized at the end of the shock tube, were focused on to a vertical slit which was resolved in time by a Hadland Industries Imacon 790 sweep camera at a rate of 5 μs/cm. An aperture and narrowband filter (589.5 nm, bandwidth 3.6 nm) were used to discriminate against flow luminosity. Timing and triggering were achieved by pressure signals from two sensors mounted in the shock-tube wall. Pulses from these transducers triggered a counter which measured the shock transit time, while the second transducer also triggered the exploding wire and streak camera, with suitable delays. The uncertainty in the measured shock speed was ± 0.05 km/s.

The optical arrangement for hook interferometry is illustrated in figure 4. The light sources used had sufficiently short pulse times (≈ 5 ns for the N_2LPDL and 500 ns for the FLPDL) to freeze the shock wave and flow. The light from the N_2LPDL was allowed to diverge through the Mach Zehnder interferometer without focusing, while that from the FLPDL system was collimated to a thin rectangular beam. The end of the test section was imaged on to the entrance slit of the spectrometer through a 90° beam rotator and lens, thus allowing spatial resolution along the direction of

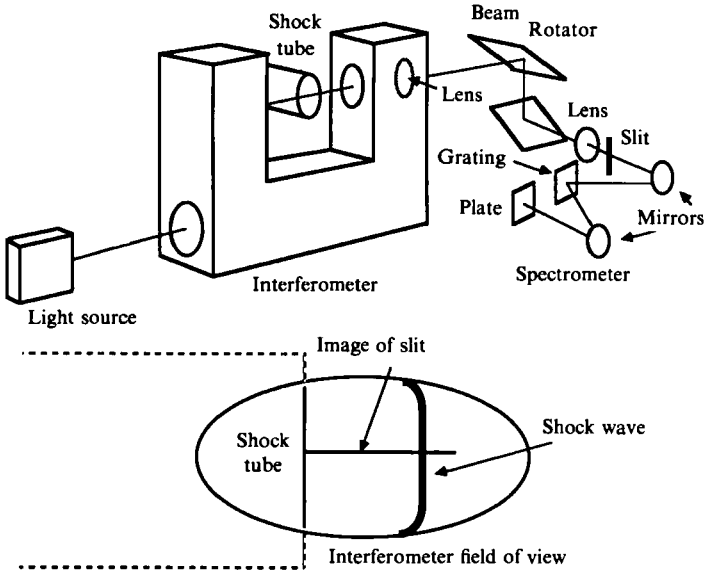

FIGURE 4. Optical arrangement for spatially resolved hook interferometry, and interferometer field of view.

the flow. The plate factor of the spectrometer was measured to be 0.76 nm/mm by using two or more emission lines from an argon-vapour lamp. These lines which were recorded on the same film before each shot were also used to identify the transition lines. Kodak high-speed infra-red film was used to obtain good exposures at the wavelengths under study. For the N_2LPDL experiments the entrance slit of the spectrometer was maintained at 100 μm, giving a spectral resolution of 0.08 nm. However, because of the greater light intensity, it was possible to decrease this to 20 μm for some of the FLPDL experiments, increasing the spectral resolution to 0.015 nm. The pressure transducer nearest the end of the tube was used as the trigger with a suitable delay for the pulsed light source. Photodiodes were used to monitor the arrival of the shock at the end of the tube and the laser pulse, to give an accurate measurement of this delay time.

4. Results and discussion

4.1. *Time-resolved interferograms*

Examples of time-resolved interferograms are shown in figures 5–7, while the conditions and classifications for each interferogram are summarized in table 1. Quoted are the shock-tube fill pressure, shock speed, relaxation length of the flow, and a classification. Four categories are used: S indicates a stable flow; D indicates a doubtful unstable electron-cascade front; U indicates an unstable electron-cascade front; and RU indicates that only the radiative recombination region is disturbed. Examples of the stable and unstable cases are shown in figure 5. In each picture the shock front (S) is evident as a positive fringe jump due to the sudden increase in density and hence refractive index. Time is increasing from right to left, and this is equivalent to the shock wave moving to the right. Behind the shock, at varying distances, is a negative fringe shift indicating the elctron cascade front (E). This is

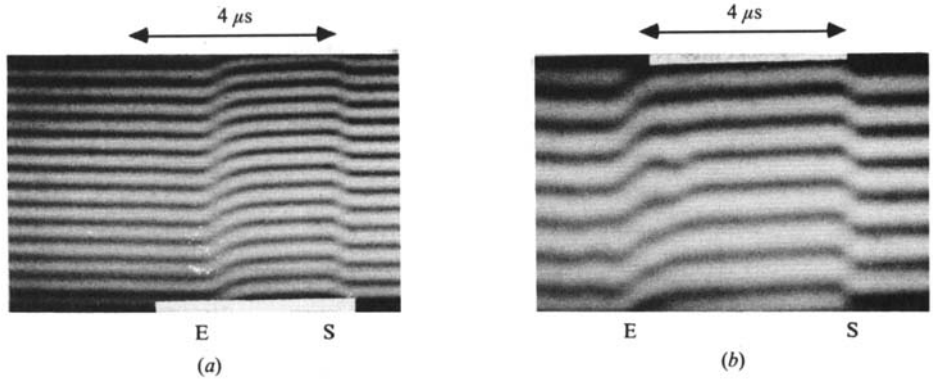

FIGURE 5. Time resolved interferograms. (*a*) Shock classified as stable. $p_0 = 5$ Torr; $u_s = 4.80$ km/s; $T_0 = 294$ K. (*b*) Shock classified as unstable. $p_0 = 5$ Torr; $u_s = 4.78$ km/s; $T_0 = 294$ K.

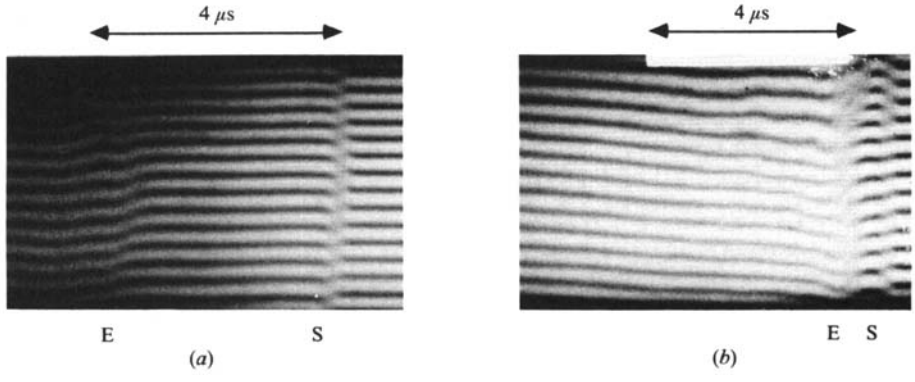

FIGURE 6. Time-resolved interferograms of unstable shock waves at $p_0 = 10$ Torr and $T_0 = 294$ K. (*a*) $u_s = 4.31$ km/s; $M_s = 13.5$. (*b*) $u_s = 5.25$ km/s; $M_s = 16.4$.

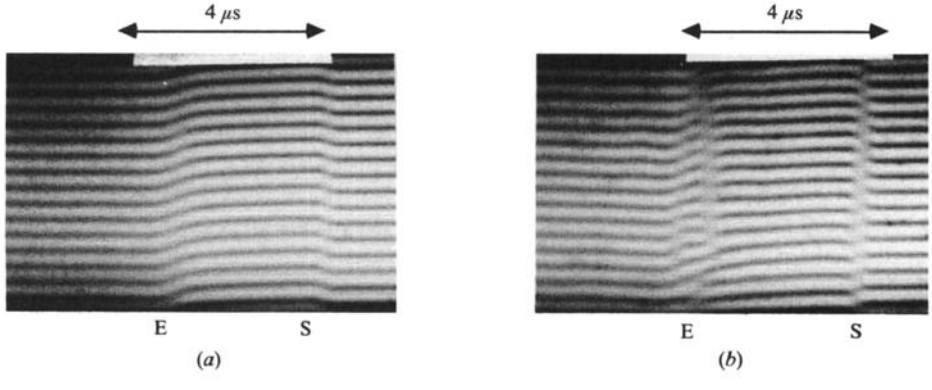

FIGURE 7. Time-resolved interferograms for shock waves at same Mach number ($M_s = 14.8$), but different filling pressures (*a*) $p_0 = 4$ Torr; (*b*) $p_0 = 10$ Torr.

p_0 ($\pm$0.5 Torr)	u_s ($\pm$0.05 km/s)	Relaxation length ($\pm$1 mm)	Classification
2.8	4.97	16	S
2.8	5.33	11	RU
2.8	5.51	10	S
2.8	5.75	7	S
4.0	4.73	14	S
5.0	4.23	29	S
5.0	4.55	28	S
5.0	4.70	19	RU
5.0	4.78	22	U
5.0	4.80	13	S
10.0	4.06	39	D
10.0	4.22	28	U
10.0	4.31	19	U
10.0	4.73	15	U
10.0	5.00	12	U
10.0	5.25	4	U

TABLE 1. Flow visualization results. Classification of stability for different filling pressures p_0 and shock speeds u_s. S indicates a stable flow, U an unstable cascade front and RU an unstable recombination region. D indicates that the stability of the flow could not be determined.

observed, since electrons have a refractive index less than unity. The region between these two shifts is the relaxation region and the zone behind the electron-cascade front is the radiative recombination region. The fringes here have a small positive slope due to the slow density increase as the gas cools because of radiation losses. Care needs to be exercised when classifying the interferograms at lower densities, since smaller flow perturbations are less evident because of the limited resolution of the interferometer. For this reason, classifications were made on the basis of the shape of the electron-cascade front, rather than fringe shifts indicating perturbations in flow density.

Figure 6 shows two interferograms at the higher initial fill pressure of 10 Torr. In each photograph the electron cascade front is perturbed and the radiative recombination region also disturbed. Table 1 allows a comparison between stability for the higher and lower filling pressures. For the initial pressures of 2.8 and 4 Torr most of the flows are stable. However, for the initial pressure of 10 Torr all the flows are somewhat disturbed. This is consistent with the proposal that density plays a crucial role in the onset of instability. A second trend observed is that the instabilities are worse for a higher shock velocity. Figure 6(*b*), the fastest shock, has a very severe perturbation of the electron-cascade front while those at lower shock speeds, such as in figure 6(*a*) are far less perturbed. Both trends are consistent with the proposal made by Mishen *et al.* (1981). An increase in density would suggest that a larger number of metastable atoms are formed and the molecular ions are deactivated at a faster rate. The stronger shock affects the energy release as it imparts more energy into the system. A further observation is that the relaxation length shortens with increasing shock velocity. This can be explained by realizing that a faster shock induces higher temperatures and densities which cause an acceleration of the reaction sequence. Mishen *et al.* also propose that at even higher densities, the flow should once again become stable, since deactivation exceeds the rate at which

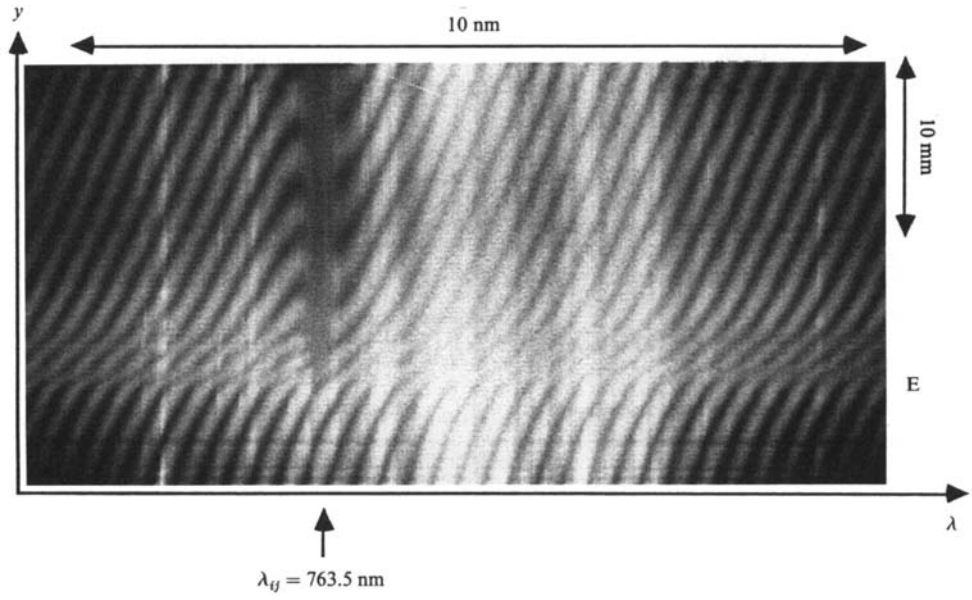

FIGURE 8. Spatially resolved hook interferogram obtained with FLPDL system. E, electron-cascade front; λ_{ij}, transition line.

metastable particles are being produced. As yet we have been unable to verify this, since at the highest densities studied in the present work the cascade front is still perturbed.

4.2. *Hook interferometry results*

The above comments, of course, are valid only if the production of metastable atoms behind the shock is a reality. To determine whether such particles are in fact produced as predicted, we study the results obtained using hook interferometry. A selected hook interferogram showing the electron-cascade front and the post-shock flow are given in figure 8. Wavelength increases from left to right, while distance from shock to electron-cascade front is from bottom to top. The absorption line λ_{ij} under consideration was marked by the corresponding emission line from an argon-vapour lamp. Fringes both before and after the shock showed no sign of the formation of hooks and thus the population of each excited level studied was less than the smallest resolvable value. The interferograms show the electron-cascade front (E) evident as a deviation of slope and a narrowing of the fringes. No hook was formed between the shock and electron-cascade front, but hooks did form within the electron-cascade front.

Comparisons between theoretical and measured populations were carried out for both stable and unstable conditions. The theoretical calculations were performed by a computer code based on the kinetic model presented by Oettinger & Bershader (1967). The theoretical values of the excited-state populations were computed via (1), and are plotted together with the experimental results in figure 9. It was considered that the more complete calculations of Meyer-Prüssner (1983) were unnecessary for the present study, since the effects of the non-Maxwellian distributions are only significant for populations far below the resolution limit of our experiment. Similarly, effects on the relaxation length are small when compared with our errors. The experimental values for the excited-sate populations were calculated from the

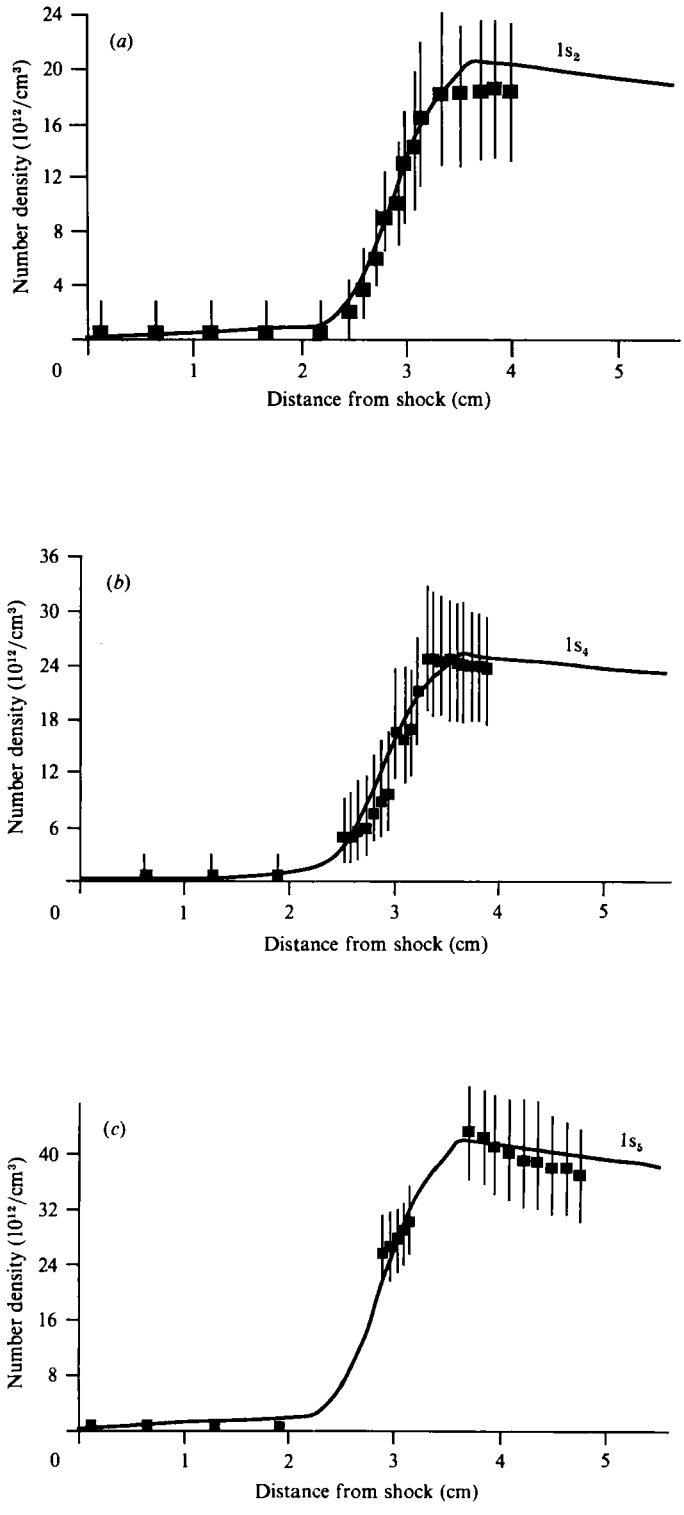

FIGURE 9(*a–c*). For caption see facing page.

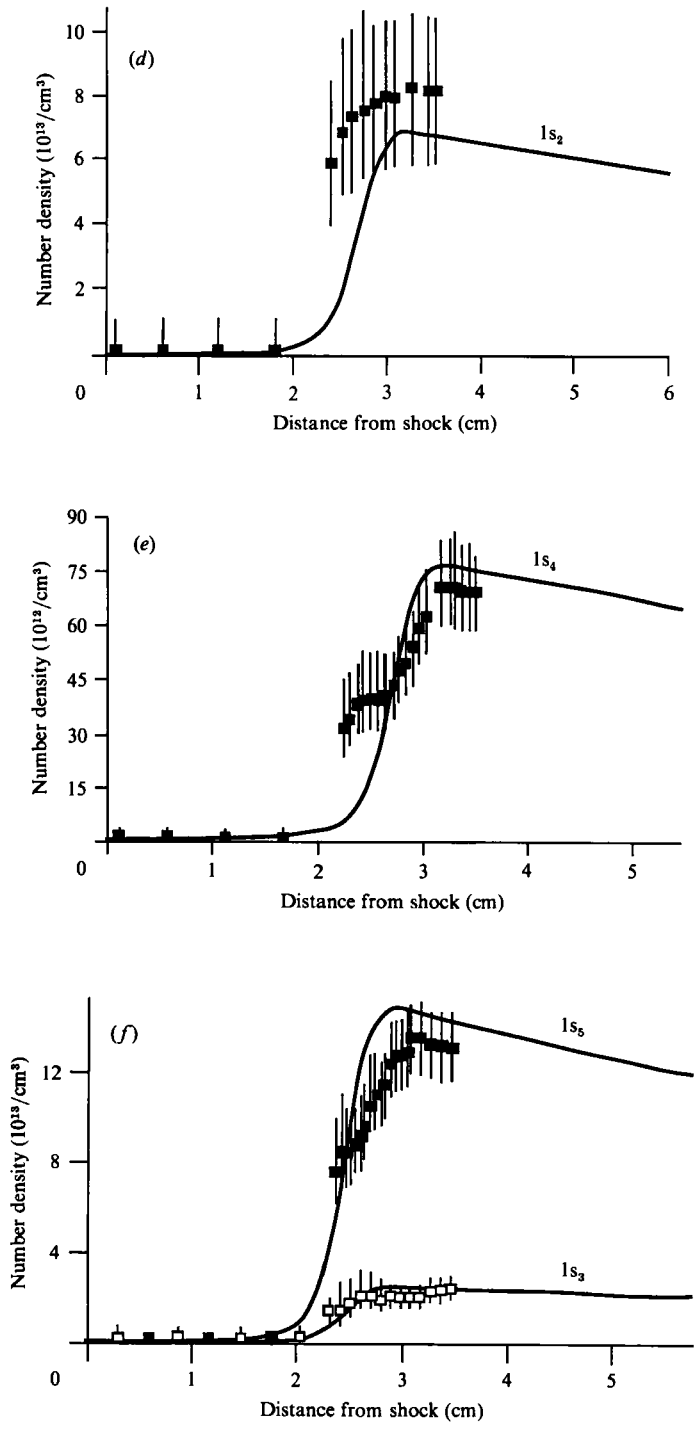

FIGURE 9. Experimental and theoretical values of excited-state populations: ——, theoretical curve; □, experimental values. (a) Stable case $1s_2$ population; (*b*) stable case, $1s_4$ population; (*c*) stable case, $1s_5$ population; (*d*) unstable case, $1s_2$ population; (*e*) unstable case $1s_4$ population; (*f*) unstable case, $1s_3$ and $1s_5$ populations. For (*a*)–(*c*) $p_0 = 2.8$ Torr, $u_s = 4.82$ km/s, while for (*d*)–(*f*) $p_0 = 10$ Torr, $u_s = 4.35$ km/s.

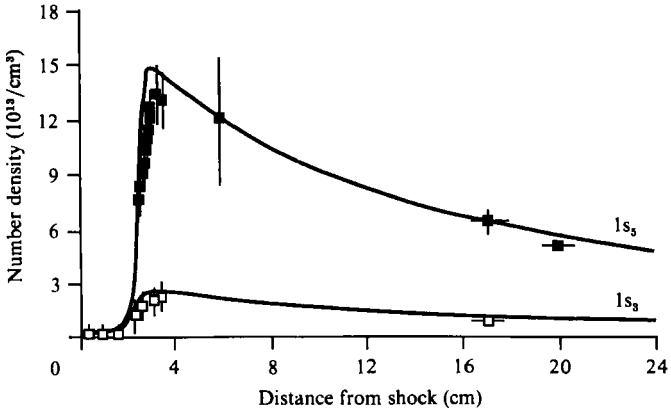

FIGURE 10. Experimental and theoretical values of metastable populations in relaxation zone and quasi-equilibrium region. $p_0 = 10$ Torr, $u_s = 4.35$ km/s.

measured hookwidths via (3) and (4). It was possible to measure the populations of the $1s_2$, $1s_4$ and $1s_5$ levels independently. However, in order to determine the $1s_3$ population, it was necessary to de-convolute the 772.376 and 772.421 nm lines. Errors in determining the excited-state populations were mainly due to the limits placed on the spectral resolution through the width of the spectrometer entrance slit. There was, however, also a small contribution from errors in locating the hook positions on the interferograms. The error bars associated with points at zero number density indicate the smallest resolvable population for the particular transition line under study. Not included in these errors are the contributions from uncertainties in the quoted oscillator strengths.

One limitation of the present experimental arrangement is the existence of the expansion fan at the shock-tube exit, which restricts the steady flow to a Mach cone region as illustrated in figure 11. This figure depicts a ray from the interferometer test beam passing through the flow at a distance z from the edge of the shock tube. The pathlength L of this ray can be broken up into two components, $L_1 = 2r$ and $L_2 = 2r'$, where r is the radius of the Mach cone at z, and r' is the width of the annulus between the shock front and the Mach cone. The value of r can be found quite readily for a particular value of z once the Mach angle μ ia known. However, the value of r', and the values of the non-equilibrium flow parameters in the unsteady expansion, are not as easily determined. None the less, it is necessary to estimate the contribution of these parameters to the measured hookwidths. This can be done by estimating the minimum and maximum values of the excited-state population between the diffracted shock wave and the edge of the Mach cone. Furthermore, an estimate of r' can be obtained by assuming a particular shape for the diffracted shock. It is thus possible to determine a lower and upper bound for the effect of the expansion on the hookwidths. These bounds will represent systematic errors on the measured populations, the errors being smallest at the tube exit and increasing with z. Thus for a particular interferogram, the errors will be largest for small values of y and will decrease with increasing y. It is important to note, however, that the results given in each figure of figures 9 and 10 are from measured hookwidths from three or more interferograms, the electron-cascade front being at a different value of z in each case. Consequently it was possible to reduce the systematic errors for quite a number of measurements.

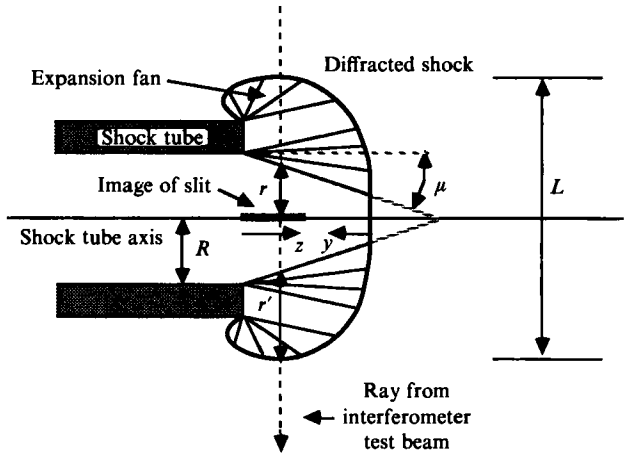

FIGURE 11. Sketch of flow at shock tube exit.

Although the prime objective of the present experimental work was to measure the excited-state populations inside the relaxation zone, some measurements were also made of metastable populations in the radiative recombination region. These measurements were for the purpose of determining whether collisional de-excitation of these levels was sufficiently fast to keep pace with the cooling process. It was possible to use a slightly different experimental arrangement which improved the resolution of the excited-state populations for these latter measurements, since it was not necessary to have the same degree of spatial resolution that was required when determining populations inside the relaxation zone. The results from these experiments are plotted in figure 10, together with some values from figure 9(*f*).

From figure 9, we note that the values predicted by Oettinger & Bershader (1967) are in excellent agreement with our experimental measurements for both the stable and unstable cases. However, on comparing the results of figure 9 with the predictions of figure 1, we note that metastable populations predicted on the basis of Yushchenkova's rate equation are about 50 times larger than those based on (1) and our experimental values. Our results therefore indicate that reaction (0) proceeds at a much slower rate than predicted, and that the anomalously high populations are not reached. One might argue that, since the metastable population reaches an appreciable value at the electron-cascade front, an amended form of the reaction scheme (0) to (II) could occur at the electron-cascade front or in the radiative recombination region. However, we are sceptical about such a proposal, for the following reason: the whole concept of anomalous relaxation is based on the assumption that the excitation temperature of the metastable particles is much larger than the Maxwellian temperature of the flow. In contrast, our experimental results have shown that the metastable populations in the quasi-equilibrium region are consistent with the predictions of Oettinger & Bershader (see figure 10), thus suggesting that these populations are in equilibrium with the flow, and consequently there is no energy available for de-excitation.

5. Conclusions

We have demonstrated that the atom–atom collisional process suggested by Yushchenkova (1980) is not an efficient means of populating the metastable states since their populations were shown to be unresolvable in the relaxation zone. However, since they were considerably higher at the electron-cascade front, we deduce that electron–atom collisions are more efficient in populating these levels. This point is consistent with the accepted theory of excitation and ionization of argon, but contradicts the proposed reaction scheme for destabilizing the shock wave. In addition, our experiments have further substantiated the two-step ionization process for argon, since the results indicate that the populations of the levels studied are consistent with Boltzmann distributions based on the electron temperature.

We would like to thank Dr H. Bachor for many fruitful discussions during the course of this research. We also acknowledge the work of Mr B. Chadwick and Mr E. Mägi, who undertook extensive preliminary investigation with the FLPDL system to obtain the desired fluorescence output in the near infra-red. We are also grateful to Mr G. Davis for his competent operation of the shock tube, and to Mr K. Lovegrove for his assistance with photographic work. Part of this work was supported by an ARGS Research Grant.

REFERENCES

BARYSHNIKOV, A. S. & SKVORTSOV, G. E. 1979 *Zh. tekh. Fiz.* **49**, 2383–2485.

BATES, D. R., KINGSTON, A. E. & MCWHIRTER, R. W. P. 1962 *Proc. R. Soc. Lond.* A**267**, 297–312.

BOND, J. W. 1957 *Phys. Rev.* **105** (6), 1683.

BRISTOW, M. P. F. & GLASS, I. I. 1972 *Phys. Fluids* **15**, 2066.

BROWN, E. A. & MULLANEY, J. 1964 *Am. Phys. Soc., Div. Fluid Dyn. Meeting, California.*

BYRON, S., STABLER, R. C. & BORTZ, P. I. 1962 *Phys. Rev. Lett.* **8**, 376–379.

DEMMIG, F. 1977 *Proc. 11th Intl Shock Tube Symp., Seattle.*

DEMMIG, F. 1983 *Proc. 14th Intl Symp. Shock Tubes and Waves, Sydney.*

D'YAKOV, S. P. 1954 *Zh. eksp. teor. Fiz.* **27**, 288–295.

ERPENBECK, J. J. 1963 *Ninth Symposium (International) on Combustion* , pp. 442–453. Academic.

ERPENBECK, J. J. 1969 *Twelfth Symposium (International) on Combustion*, pp. 711–721. Pittsburgh: The Combustion Institute.

FICKETT, W. & DAVIS, W. C. 1979 *Detonation.* University of California Press.

FREEMAN, N. C. 1955 *Proc. R. Soc. Lond.* A**228**, 341–362.

FREEMAN. N. C. 1957 *J. Fluid Mech.* **2**, 397.

GLASS, I. I. & LIU, W. S. 1978 *J. Fluid Mech.* **84** (1), 55–77.

GLASS, I. I. & PATTERSON, G. N. 1955 *J. Aero. Sci.* **22** (2), 73–100.

GRIFFITHS, R. W., SANDEMAN, R. J. & HORNUNG, H. G. 1976 *J. Phys*, D: *Appl. Phys.* **8**, 1681.

HARWELL, K. E. & JAHN, R. G. 1964 *Phys. Fluids* **7** (2), 214.

KELLY, A. J. 1966 *J. Chem. Phys.* **45** (5), 1723.

LAPWORTH, K. C. 1959 *J. Fluid Mech.* **6**, 469.

MCLAREN, T. I. & HOBSON, R. M. 1968 *Phys. Fluids* **11** (10), 2162.

MARLOW, W. C. 1967 *Appl. Optics* **6**, 1715.

MEISSNER, K. W. 1926 *Z. Phys.* **39**, 172.

MEISSNER, K. W. & GRAFFUNDER, W. 1927 *Annln. Phys.* **84**, 1009.

MEYER-PRÜSSNER, R. 1983 Dissertation, Universität Hannover.

MISHIN, G. I., BEDIN, A. A. P., YUSHCHENKOVA, N. I., SKVORTSOV, G. E. & RYAZIN, A. P. 1981 *Zh. tekh. Fiz.* **51**, 2315–2324.

VON MOORHEIM, W. K. & GEORGE, A. R. 1975 *J. Fluid Mech.* **68**, 97–108.

MORGAN, E. J. 1964 *Am. Phys. Soc. Div. Fluid Dyn. Meeting, California.*

OETTINGER, P. E. & BERSHADER, D. 1967 *AIAA J.* **5** (9), 1625–1632.

PETSCHEK, H. & BYRON, S. 1957 *Ann. Phys.* **1** (3), 270.

PHELPS, A. V. & MOLNER, J. P. 1953 *Phys. Rev.* **89** (6), 1202–1208.

PIERCE, B. M. & BIRGE, R. R. 1982 *IEEE J. Quantum. Electron.* **QE-18** (7), 1164.

SANDEMAN, R. J. 1979 *Appl. Optics* **18**, 3873.

SANDEMAN, R. J. & ALLEN, G. H. 1971 *Proc. 8th Int. Shock Tube Symp.* Chapman & Hall,

SANDEMAN, R. J. & EBRAHIM, N. A. 1977 *Appl. Optics* **16**, 1376.

WEISE, W. L., SMITH, M. W. & MILES, B. M. 1969 *Atomic Transition Probabilities, Nat. Bur. Stand. (US)* **22**, 193.

WEYMANN, H. D. 1958 *Inst. Fluid Dyn. Appl. Math. Univ. of Maryland*, TN no. BN-144.

WHITHAM, G. B. 1956 *J. Fluid Mech.* **2**, 145–171.

WONG, H. & BERSHADER, D. 1966 *J. Fluid Mech.* **26** (3), 459.

YUSHCHENKOVA, N. I. 1980 *Pis'ma Zh. Tekh. Fiz.* **6**, 1283.